THE ASTROPHYSICAL JOURNAL, 494:691–699, 1998 February 20

DIFFERENTIAL ROTATION AND MERIDIONAL FLOW FOR FAST-ROTATING SOLAR-TYPE STARS

GÜNTHER RÜDIGER,[1] BRIGITTA VON REKOWSKI,[1] ROBERT A. DONAHUE,[2,3] AND SALLIE L. BALIUNAS[2,3,4]

Received 1996 December 9; accepted 1997 October 1

ABSTRACT

Observations indicate that normalized surface differential rotation *decreases* for fast-rotating stars, that is, $|\Delta\Omega|/\Omega \propto \Omega^{-0.3}$. An *increase* of $|\Delta\Omega|/\Omega$ is provided, however, by the current Reynolds stress theory of differential rotation in stellar convection zones, without the inclusion of meridional flow. We compute both the pole-equator difference of the surface angular velocity and the meridional drift for various Taylor numbers to demonstrate that the inclusion of meridional flow in the computations for fast rotation yields a systematic reduction of the resulting differential rotation. Our model's adiabatic and density-stratified convection zone, with stress-free surfaces and a thickness of 0.3 stellar radii, yields the relation $|\Delta\Omega|/\Omega \propto \Omega^{-(0.15 \dots 0.30)}$ for stars with faster rotation than the Sun, in agreement with previous observations. If the Coriolis number rather than the Taylor number is varied, we find a maximum differential rotation of 20%. For stars with fast rotation, exponents of up to $n' \simeq 0.4$ are found. All rotation laws exhibit superrotating equators.

Subject headings: hydrodynamics — stars: rotation — turbulence

1. MOTIVATION

Recent developments have been made in the observational study of surface differential rotation. Donahue (1993) used the long-term database of chromospheric activity measurements from the Mount Wilson Observatory HK Project to monitor changes in the seasonal rotation period of lower main sequence stars. From a sample of 110 stars, 36 had five or more determinations of rotation period over the twelve years of data available. For some of these stars, there is evidence of trends between rotation period and level of activity, or, where measurable, activity cycle phase (Baliunas et al. 1995).

While some slow-rotating stars ($P_{\rm rot} > 10$ days) show an equatorward migration pattern that is similar to the Sun's, the opposite situation, in which $P_{\rm rot}$ *increases* with activity cycle phase, is clearly present in several stars (Donahue 1993; Donahue & Baliunas 1994), even some with similar spectral type (i.e., mass) and mean rotation period (i.e., age). This "antisolar" pattern could reflect either a poleward migration of active regions against a solar-like surface differential rotation, or possibly the presence of poleward acceleration. A few stars, for example β Comae, may have two active latitude bands (Donahue & Baliunas 1992; however, Gray & Baliunas 1997 offer a different explanation), although for several of these stars the range of periods observed within each activity band is very small, $<2\%$ (e.g., χ^1 Ori; Donahue & Baliunas 1994). Young stars (<1 Gyr) tend to have no discernible pattern of seasonal rotation period with either time or mean level of surface activity.

For all the stars studied, the range of rotation period observed, ΔP, increases with the mean rotation period, $\langle P_{\rm rot} \rangle$. There is a power-law relationship,

$$|\Delta P| \propto \langle P_{\rm rot} \rangle^{1.3} , \quad (1)$$

independent of spectral type (Donahue, Saar, & Baliunas 1996). However, for stars with similar Rossby numbers, K-type stars have larger $|\Delta P|$ than G-type stars.

It is possible to explain the observed internal solar rotation by means of a Reynolds stress theory, which will determine the influence of the basic rotation on the cross correlations of the turbulent convection (Küker, Rüdiger, & Kitchatinov 1993). In a pure Reynolds stress theory, the meridional flow in such calculations is completely neglected. The reason for this omission is twofold. First, the observations only provide a slow *poleward* flow, with an amplitude of 10 m s^{-1}. It is assumed that such a slow flow only modifies the results of the Reynolds stress theory. On the other hand, inspection of the (observed) rotational isolines does not suggest a strong influence from meridional flow with one or two large cells.

The meridional circulation tends to align the isolines of angular momentum with the streamlines of the flow (cf. Rüdiger 1989; Brandenburg et al. 1990). Thus, the existence of distinct equatorial acceleration indicates that any possible meridional surface drift cannot be too strong. In the other case, because of the small distance between the polar regions and the rotational axis, it should be more likely that a polar acceleration ("polar vortex") will appear.

Moreover, for very large Taylor numbers, the flow system approaches the Taylor-Proudman state, in which the isolines are two-dimensional with respect to the rotation axis, i.e., where there is no variation along the rotational (z) axis. At the same time, the meridional circulation breaks, i.e.,

$$\frac{\partial\Omega}{\partial z} = 0 , \quad \boldsymbol{u}^m = 0 \quad (2)$$

(cf. Köhler 1969; Tassoul 1978). The first of these conditions is not seen for the Sun; the solar Taylor number, however, is large. From the definition of the Taylor number as

$${\rm Ta} = \frac{4\Omega^2 R^4}{\nu_T^2} , \quad (3)$$

with R being the stellar radius and Ω the rotation rate, and using the following reference value for the eddy viscosity,

$$\nu_T = c_\nu \, l_{\rm corr}^2/\tau_{\rm corr} \quad (4)$$

[1] Astrophysikalisches Institut Potsdam, An der Sternwarte 16, D-14482 Potsdam, Germany; gruediger@aip.de, bvrekowski@aip.de.
[2] Harvard-Smithsonian Center for Astrophysics, 60 Garden St., Cambridge, MA 02138; donahue@cfa.harvard.edu, baliunas@cfa.harvard.edu.
[3] Mount Wilson Institute, 740 Holladay Road, Pasadena, CA 91106.
[4] Center for Automated Space Science and Center of Excellence in Information Systems, Tennessee State University, 330 10th Avenue North, Nashville, TN 37203.

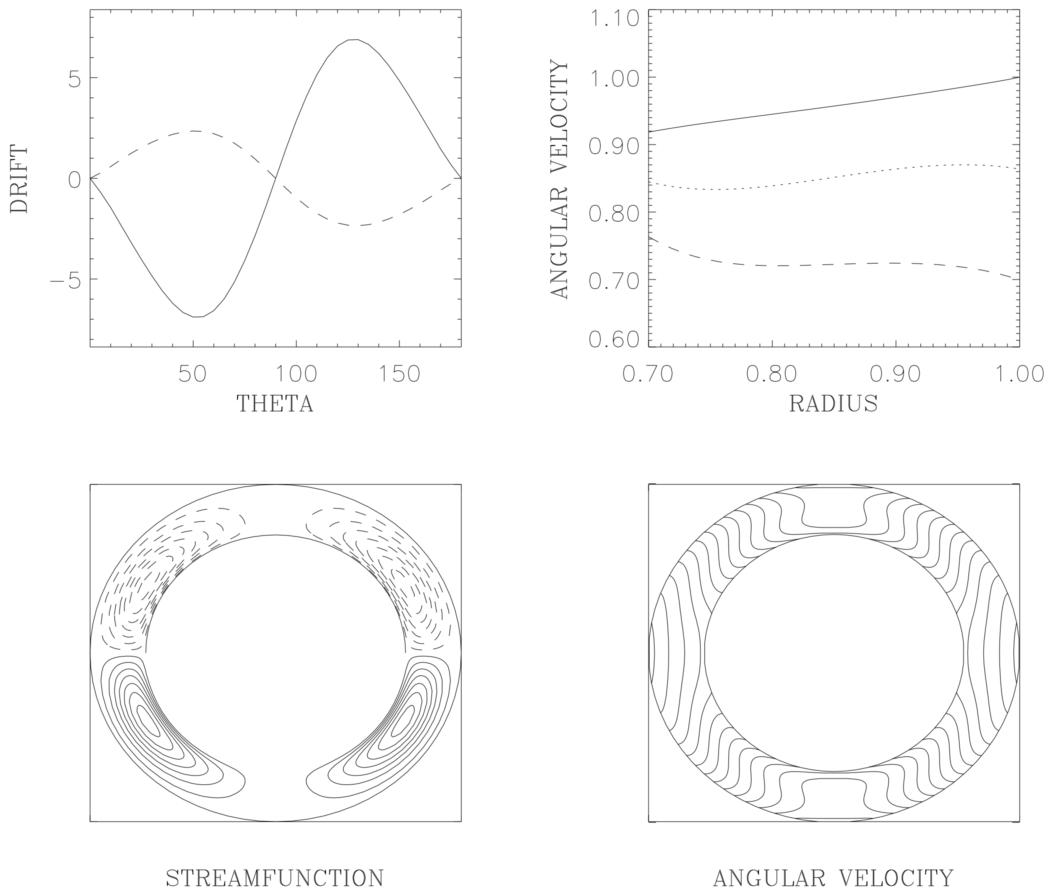

FIG. 1.—Meridional flow and differential rotation in the solar convection zone. The fixed Λ effect is from eq. (15), the Taylor number is 2×10^5, and $\alpha_{\rm MLT} = 5/3$. *Left panels*: Meridional flow in amplitude (*top*) and cell pattern (*bottom*). Amplitudes are given at the top (*solid line*) and the bottom (*dashed line*) of the convection zone. *Right panels*: Differential rotation in amplitude (*top*) and in Ω isoline representation (*bottom*). The rotation laws are given for the equator (*solid line*), the poles (*dashed line*), and midlatitudes (45°, *dotted line*).

(where $l_{\rm corr}$ is the correlation length and $\tau_{\rm corr}$ is the correlation time), we find the relation

$$\mathrm{Ta} = \frac{\Omega^{*2}}{c_v^2\, \xi^4} \, . \tag{5}$$

Here, as usual, Ω^* is the Coriolis number,

$$\Omega^* = 2\tau_{\rm corr}\, \Omega \, , \tag{6}$$

and $\xi = l_{\rm corr}/R$ is the normalized correlation length. So,

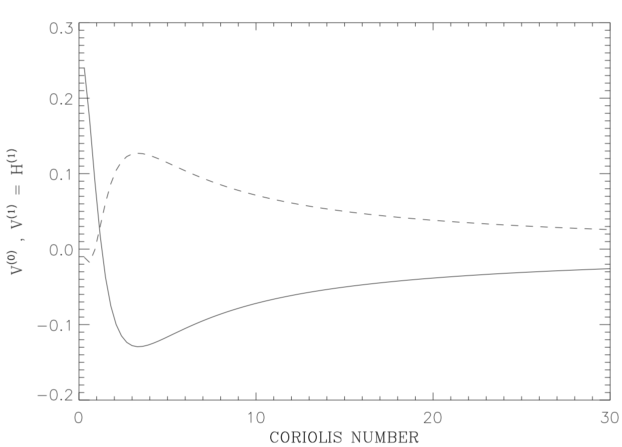

FIG. 2.—Influence of the basic rotation on the Λ effect coefficients $V^{(0)}$ (*solid line*) and $V^{(1)} = H^{(1)}$ (*dashed line*), after Kitchatinov & Rüdiger (1993).

with typically assumed values for the Sun of $\Omega^* \simeq 5$, $c_v \simeq 1$, and $\xi \simeq 0.1$ ("giant cells"), we find

$$\mathrm{Ta} \simeq 2.5 \times 10^5 \, . \tag{7}$$

With such a Taylor number, the observed differential rotation should produce a remarkable intensity in the meridional flow. Therefore, we need an additional explanation as to why the solar polar drift is so slow. Kitchatinov & Rüdiger (1995) find that the rotational influence on the eddy heat diffusion leads to a warmer pole, such that an equatorward-directed extra drift weakens the meridional circulation. Von Rekowski & Rüdiger (1997) apply the anisotropic kinetic alpha effect (Frisch, She, & Sulem 1987; Kitchatinov, Pipin, & Rüdiger 1994) to the theory of differential rotation and find both a reduction of the meridional drift and an amplified pole-equator difference in the angular velocity. In the present paper, we tune the dimensionless c_v so as to reproduce the differential solar rotation and consider it as characteristic of all rotating stellar convection zones. This philosophy is based on the general observation that the eddy viscosity of stellar envelopes only appears in the theory of differential rotation, so that it can only be measured by means of real rotation laws.

Recent analysis of observational solar data confirms the poleward direction of the flow (between 10° and 60°). Snodgrass & Dailey (1996) report a value of 13 m s^{-1}, while Hathaway (1996) derives 20 m s^{-1}, and occasionally larger ($\lesssim$50 m s^{-1}). While Snodgrass & Dailey used magne-

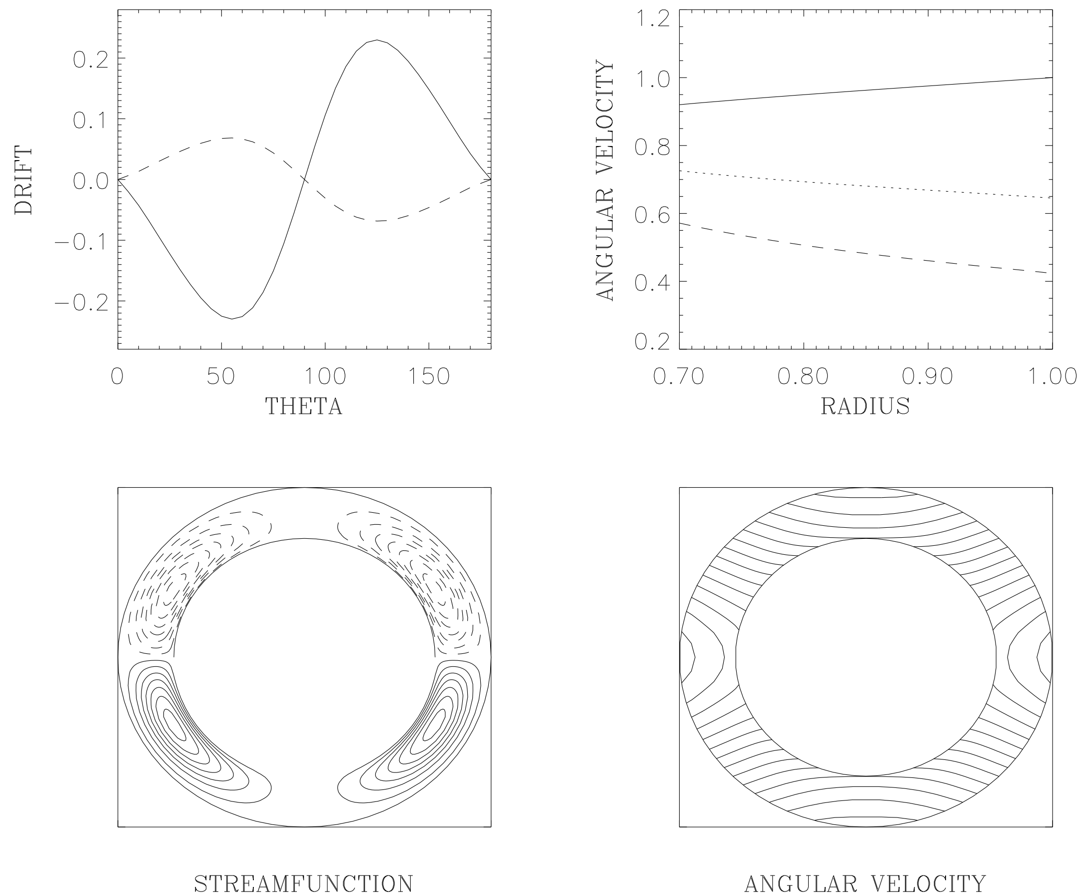

FIG. 3.—As in Fig. 1, but for slow basic rotation. The Λ parameters are fixed as in eq. (15), the Taylor number is 10^3, and $\alpha_{\mathrm{MLT}} = 5/3$.

togram data to find the meridional motions by following the motions of small magnetic features in the photosphere, Hathaway worked with Doppler velocity data obtained with the Global Oscillation Network Group (GONG) instruments. Any shortcomings that might arise through the use of magnetic tracers are thus excluded, and the results are of particular importance.

To sum up, the following strategy for this paper is proposed as reasonable: the Λ effect is prescribed in order to reproduce the "solar" case for a certain fixed Taylor number, and then the Taylor number is varied. The main question concerns the response of the surface rotation law to this procedure.

Equation (1) can also be represented as

$$\delta_{\mathrm{lat}} = \frac{|\Delta\Omega|}{\Omega_{\mathrm{eq}}} \propto \Omega^{-n'} , \quad (8)$$

with $n' = 0.3$. Recent theoretical papers that do not include meridional flow yield a negative n' value, in contrast to observations (Küker et al. 1993; Rüdiger & Kitchatinov 1996). Only by including the meridional flow in the solution of the Reynolds equation has a positive n' been found (Kitchatinov & Rüdiger 1995). This paper confirms this situation. The influence of the meridional circulation upon differential rotation is thus indirectly observed with equation (1) for fast-rotating solar-type stars.

2. TURBULENCE MODEL

A stratified turbulence can never rotate rigidly. The reason for this is that even in the case of uniform rotation—in contrast to any form of pure viscosity—the turbulence transports angular momentum. The formal description of this phenomenon is given by the nondiffusive part, Q_{ij}^{Λ}, of the correlation tensor,

$$Q_{ij} = \langle u_i'(\boldsymbol{x}, t) u_j'(\boldsymbol{x}, t) \rangle , \quad (9)$$

i.e.,

$$Q_{ij}^{\Lambda} = \Lambda_V(\epsilon_{ipk} g_j^0 + \epsilon_{jpk} g_i^0) g_p^0 \Omega_k + \Lambda_H(\boldsymbol{g}^0 \boldsymbol{\Omega}) \times (\epsilon_{ipk} \Omega_j + \epsilon_{jpk} \Omega_i) g_p^0 \Omega_k , \quad (10)$$

also called the Λ effect in Rüdiger (1989). In equation (10), $\boldsymbol{\Omega}$ is the basic rotation, while $\boldsymbol{g}^0$ gives the unit vector in radius.

According to equation (10), the turbulent fluxes of angular momentum can be written as

$$Q_{r\phi} = \cdots + \nu_T (V^{(0)} + V^{(1)} \sin^2 \theta) \Omega \sin \theta ,$$
$$Q_{\theta\phi} = \cdots + \nu_T H^{(1)} \sin^2 \theta \Omega \cos \theta , \quad (11)$$

where the coefficients $V^{(0)}$, $V^{(1)}$, and $H^{(1)}$ are functions of the Coriolis number and the density scale height,

$$H_\rho = |\boldsymbol{G}|^{-1} , \quad (12)$$

with

$$\boldsymbol{G} = \nabla \log \rho . \quad (13)$$

The elisions in equation (11) denote the contributions of the eddy viscosity tensor Q_{ij}^{ν}, which in the simplest (axisymmetric) case yields

$$Q_{r\phi} = -\nu_T r \frac{\partial \Omega}{\partial r} \sin \theta + \cdots ,$$
$$Q_{\theta\phi} = -\nu_T \frac{\partial \Omega}{\partial \theta} \sin \theta + \cdots . \quad (14)$$

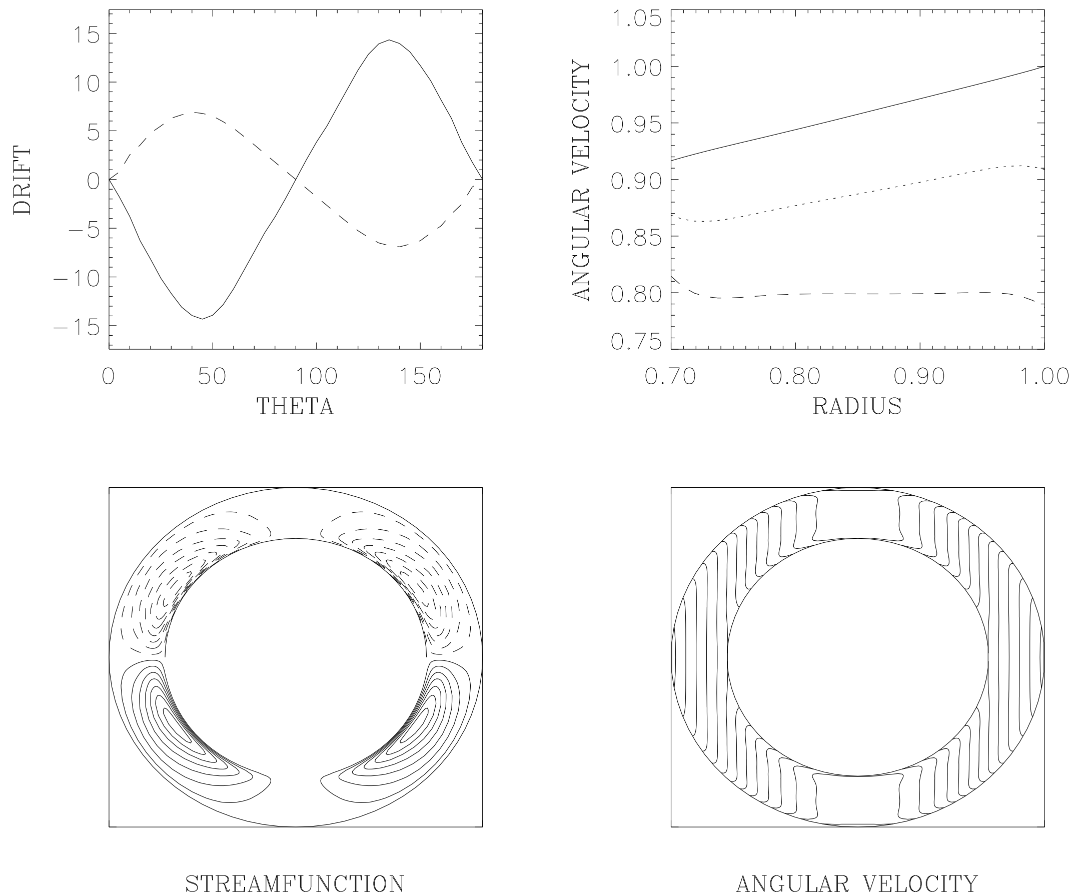

FIG. 4.—As in Fig. 1, but for rapid basic rotation. The Λ parameters are fixed as in eq. (15), the Taylor number is 10^7, and $\alpha_{\rm MLT} = 5/3$.

Küker et al. (1993), using a model of the solar convection zone from Stix & Skaley (1990), were able to reproduce the main features of the "observed" internal rotation of the Sun's outer envelope. They neglected, however, the angular momentum transport of meridional flows and magnetic fields. A simple example of a theory of differential solar rotation is given in Figure 1, produced with the numbers

$$V^{(0)} = -1 \, , \quad V^{(1)} = H^{(1)} = 1.25 \tag{15}$$

(Rüdiger & Tuominen 1990; Brandenburg et al. 1990). Again, the known principal features of the solar rotation are well reproduced. Note the disk-like structure of the Ω isocontours at the poles and the cylinder-like structure of the Ω isocontours at the equator. In midlatitudes, the angular velocity of the rotation does not vary with depth.

The main finding of Kitchatinov & Rüdiger (1993) was the representation of the functions V and H as

$$V^{(0)} = \frac{\tau_{\rm corr}^2 u_T^2}{H_\rho^2} \left[\mathscr{I}_0(\Omega^*) + \mathscr{I}_1(\Omega^*)\right] , \tag{16}$$

$$V^{(1)} = H^{(1)} = -\frac{\tau_{\rm corr}^2 u_T^2}{H_\rho^2} \mathscr{I}_1(\Omega^*) , \tag{17}$$

where $u_T = \langle \boldsymbol{u}'^2 \rangle^{1/2}$ is the rms turbulent velocity, $\tau_{\rm corr}$ is the eddy turnover time, and H_ρ is the density scale height. We adopt the approximation

$$\tau_{\rm corr}^2 u_T^2 \simeq l_{\rm corr}^2 \simeq \left(\frac{\alpha_{\rm MLT}}{\gamma}\right)^2 H_\rho^2 , \tag{18}$$

with $\alpha_{\rm MLT}$ from the usual mixing length relation

$$l_{\rm corr} = \alpha_{\rm MLT} H_p \tag{19}$$

between the mixing length, $l_{\rm corr}$, and the pressure scale height, H_p. The adiabaticity index is γ. For $\alpha_{\rm MLT} = \gamma$, we find $l_{\rm corr} = H_\rho$.

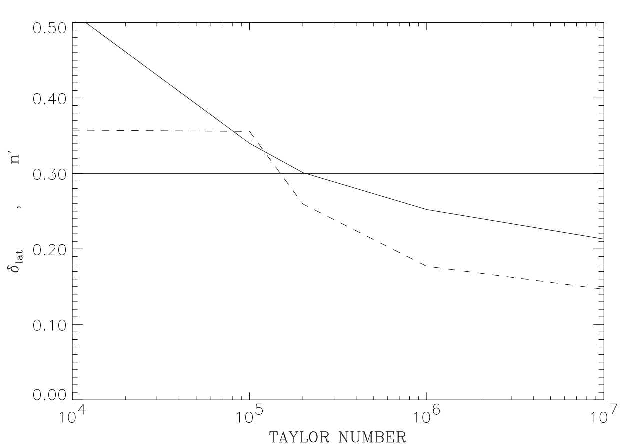

FIG. 5.—Resulting surface rotation laws for fixed Λ parameters after eq. (15), but for various Taylor numbers. *Solid line*: Influence of the Taylor number on the normalized pole-equator difference of the surface angular velocity. *Dashed line*: Exponent n' in eq. (8), scaling the normalized differential surface rotation. The observed value of 0.3 is separately marked.

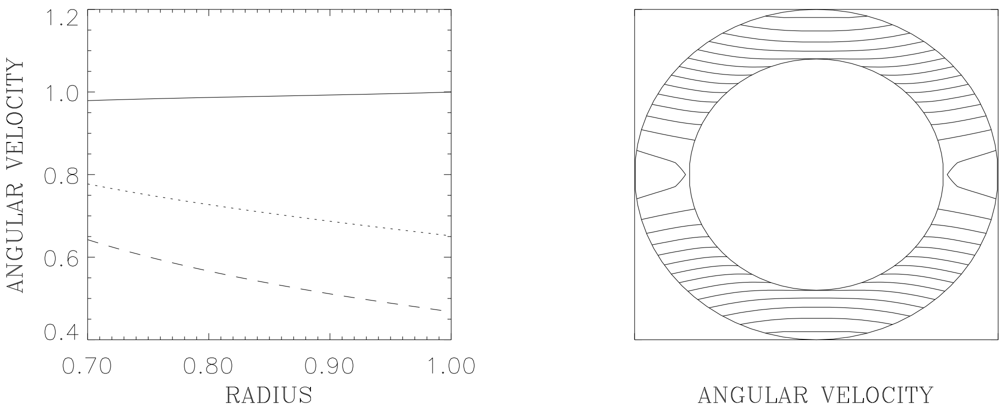

FIG. 6.—A flow-free reference status for the model family with varying Ω^*. Here $\Omega^* = 2$ and $\alpha_{MLT} = 2.5$. To suppress the angular momentum transport by meridional circulation, we have artificially set Ta = 0.

The expressions for $\mathscr{I}_0$ and $\mathscr{I}_1$ are

$$\mathscr{I}_0 = \frac{1}{2\Omega^{*4}}\left(9 - \frac{2\Omega^{*2}}{1+\Omega^{*2}} - \frac{\Omega^{*2}+9}{\Omega^*} \arctan \Omega^*\right) \quad (20)$$

and

$$\mathscr{I}_1 = -\frac{1}{2\Omega^{*4}}\left(45 + \Omega^{*2} - \frac{4\Omega^{*2}}{1+\Omega^{*2}} + \frac{\Omega^{*4} - 12\Omega^{*2} - 45}{\Omega^*} \arctan \Omega^*\right) . \quad (21)$$

These functions describe the rotation-rate dependence of the Λ effect. In Figure 2, the rotational profiles of the functions $V^{(0)}$ and $V^{(1)} = H^{(1)}$ are given. For late-type main-sequence stars, the Coriolis number Ω^* exceeds unity. In that case, indeed, the values in equation (15) give a good representation of the Λ effect. However, one has to incorporate the meridional flow into the theory. To this end, one needs to know the influence of rotation on the turbulent heat transport. If this is known from an established turbulence theory, then one can compute the complete fields of pressure, circulation, and differential rotation.

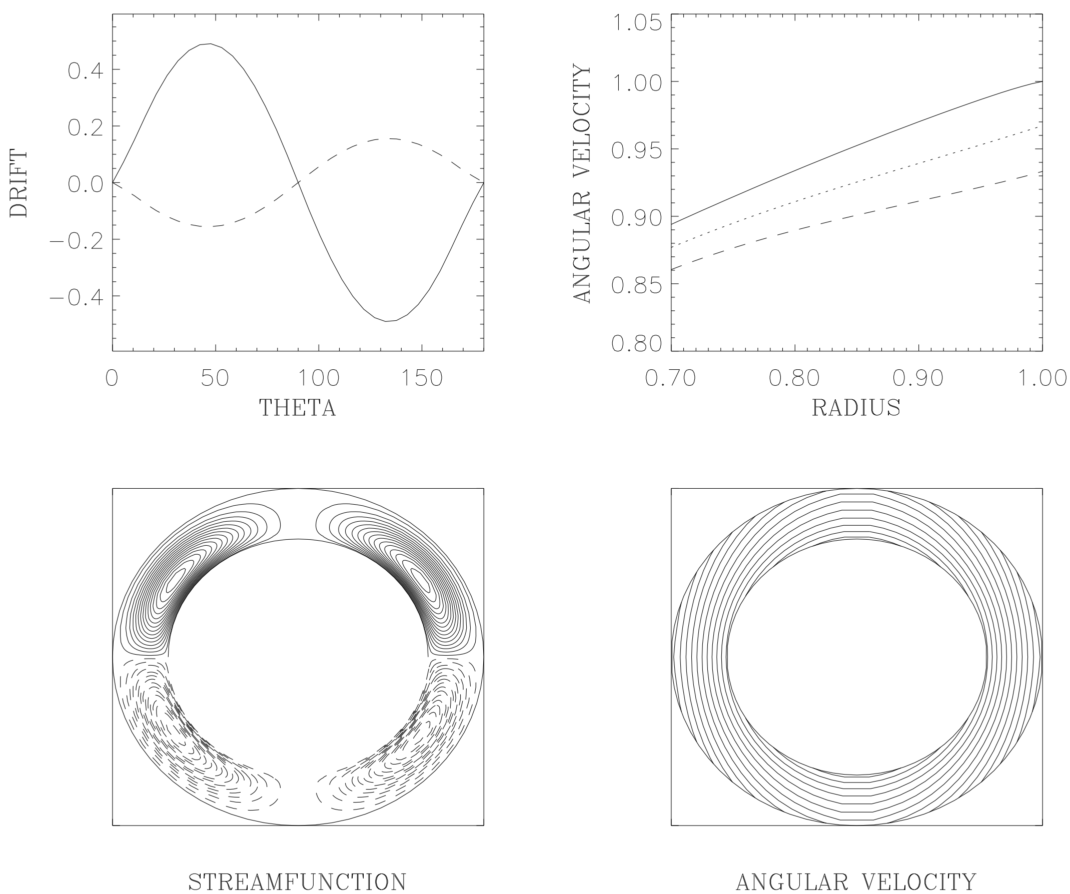

FIG. 7.—Meridional flow and differential rotation in a convection zone with $\Omega^* = 1$ (slow rotation). *Left panels*: Meridional flow in amplitude (*top*) and cell pattern (*bottom*). The amplitudes are given at the top (*solid line*) and the bottom (*dashed line*) of the convection zone. *Right panels*: Differential rotation in amplitude (*top*) and in Ω isoline representation (*bottom*). Rotation laws are given for the equator (*solid line*), the poles (*dashed line*), and for midlatitudes (45°, *dotted line*).

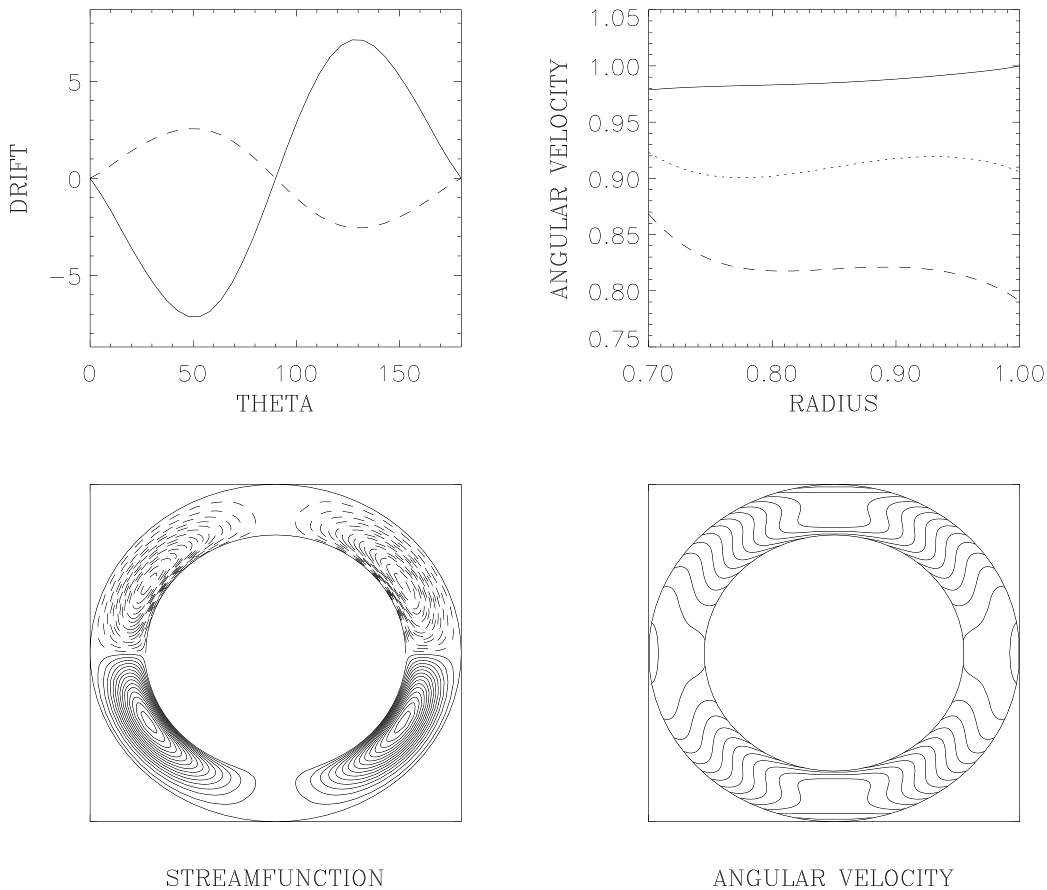

FIG. 8.—As in Fig. 7, but for moderate basic rotation, $\Omega^* = 2$

3. BASIC EQUATIONS

We solve the stationary Reynolds equation for a turbulent flow in the inertial system,

$$(\bar{\boldsymbol{u}}\nabla)\bar{\boldsymbol{u}} + \frac{1}{\rho}\,\mathrm{Div}\,(\rho Q) + \frac{\nabla p}{\rho} = \boldsymbol{g}\,. \tag{22}$$

The tensor divergence Div (ρQ) is a vector with the components $\partial(\rho Q_{ij})/\partial x_j$. Here $\boldsymbol{g}$ denotes the gravity acceleration, which is assumed to be uniform. Magnetic fields and deviations from the axisymmetry are not considered. Only anelastic fluids are considered, i.e.,

$$\mathrm{div}\,(\rho\bar{\boldsymbol{u}}) = 0\,. \tag{23}$$

After adopting these initial assumptions, the *azimuthal* component of equation (22) is given by

$$\frac{\partial}{\partial x_j}\,[\rho r \sin\theta(\bar{u}_j\bar{u}_\phi + Q_{j\phi})] = 0\,. \tag{24}$$

Our energy equation might be overly simple. The turbulence is considered to be so intensive that the medium will be isentropic,

$$S = C_v \log\,(p\rho^{-\gamma}) = \mathrm{const}\,, \tag{25}$$

hence, there is a direct relation between density and pressure. If this is true, the pressure term in equation (22) can be written as a gradient that disappears after application of curling:

$$\mathrm{curl}_\phi\left[(\bar{\boldsymbol{u}}\nabla)\bar{\boldsymbol{u}} + \frac{1}{\rho}\,\mathrm{Div}\,(\rho Q)\right] = 0\,. \tag{26}$$

It remains to fix the flow field by

$$\bar{u}_r = \frac{1}{\rho r^2 \sin\theta}\,\frac{\partial A}{\partial\theta}\,,\quad \bar{u}_\theta = -\frac{1}{\rho r \sin\theta}\,\frac{\partial A}{\partial r}\,,$$
$$\bar{u}_\phi = \Omega_0\, r\sin\theta + u_\phi\,. \tag{27}$$

For normalization, we use the relations

$$r = Rx\,,\quad \rho = \rho_*\hat{\rho}\,,\quad A = \rho_* R\nu_T\hat{A}\,,\quad u_\phi = R\Omega_0\,\hat{u}_\phi\,, \tag{28}$$

i.e.,

$$\bar{u}_r = \frac{\nu_T}{R}\,\hat{\bar{u}}_r\,,\quad \bar{u}_\Theta = \frac{\nu_T}{R}\,\hat{\bar{u}}_\Theta\,,\quad \bar{u}_\phi = R\Omega_0\,\hat{\bar{u}}_\phi\,. \tag{29}$$

The density stratification from equation (13) is then represented by

$$H_\rho = -\frac{dr}{d\log\rho} = R\hat{H}\,. \tag{30}$$

For the conservation law of the angular momentum, we get the dimensionless equation

$$\frac{1}{x^2}\frac{\partial}{\partial x}\,(x^2\hat{\rho}\hat{Q}_{\phi r}) + \frac{1}{x\sin\theta}\frac{\partial}{\partial\theta}\,(\sin\theta\,\hat{\rho}\hat{Q}_{\phi\theta})$$
$$+\frac{\hat{\rho}}{x}\,\hat{Q}_{r\phi} + \frac{\hat{\rho}\cot\theta}{x}\,\hat{Q}_{\theta\phi} + 2\hat{\rho}\cos\theta\left(-\frac{1}{\hat{\rho}x\sin\theta}\frac{\partial\hat{A}}{\partial x}\right)$$
$$+\,2\hat{\rho}\sin\theta\left(\frac{1}{\hat{\rho}x^2\sin\theta}\frac{\partial\hat{A}}{\partial\theta}\right) = 0\,. \tag{31}$$

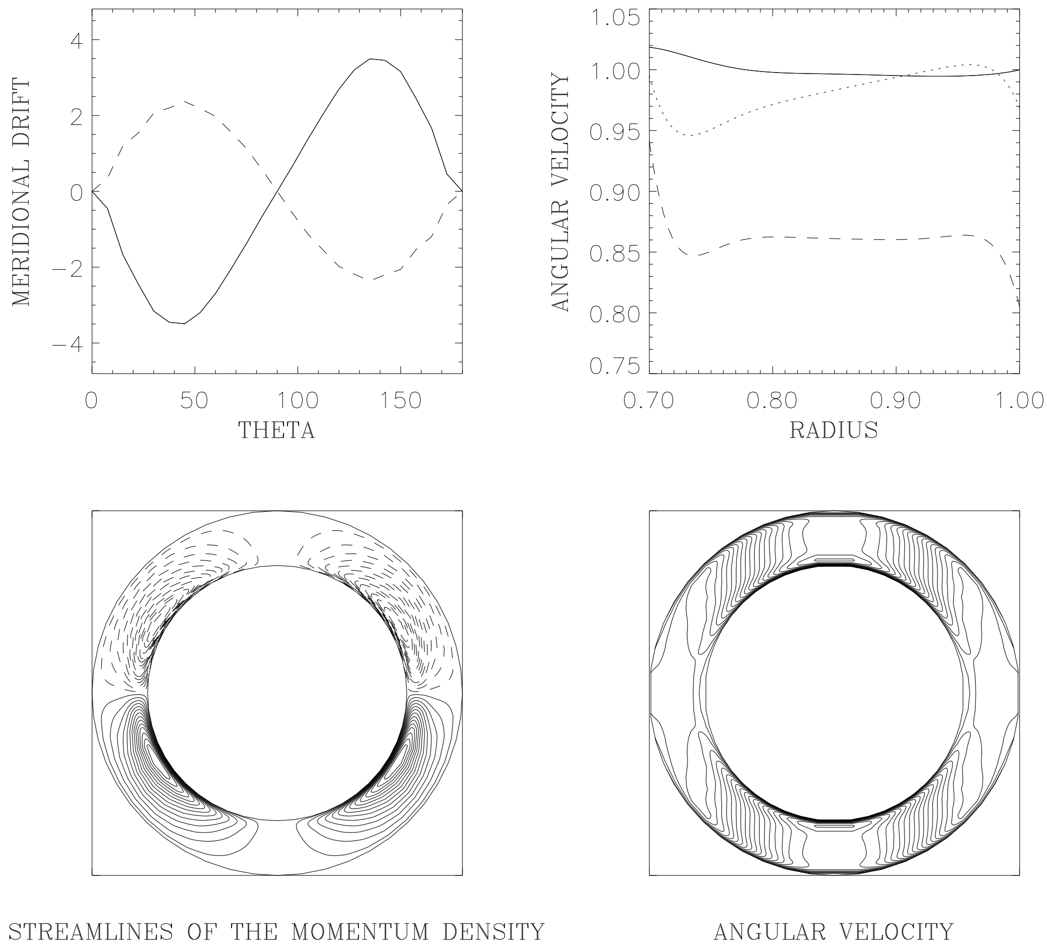

FIG. 9.—As in Fig. 7, but for fast basic rotation, $\Omega^* = 5$

Here also the turbulent fluxes of angular momentum are written in dimensionless form, in accordance with

$$Q_{i\phi} = \nu_T \Omega_0 \hat{Q}_{i\phi} , \quad i = r, \theta . \qquad (32)$$

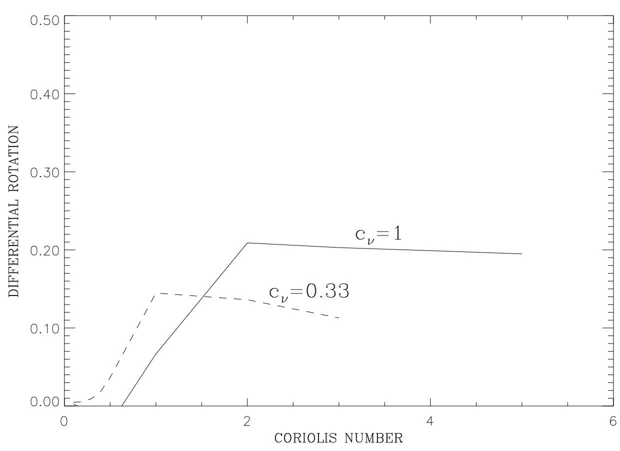

FIG. 10.—Normalized differential surface rotation scaled with the basic rotation rate for different values of the viscosity parameter c_ν given in eq. (4). Note the existence of maxima of differential rotation for each c_ν value. For faster rotation, the meridional flow smoothes the surface rotation law ($l_{\rm corr}/R = 0.1$, $\alpha_{\rm MLT} = 2.5$).

Equation (31) is linearized by means of the assumption

$$|u_\phi| \ll \Omega_0 R . \qquad (33)$$

The meridional equation is formulated under the same condition. Hence, the "centrifugal force" is reformulated as

$$\bar{u}_\phi^2 \simeq r^2 \sin^2 \theta \Omega_0^2 + 2r \sin \theta \Omega_0 u_\phi . \qquad (34)$$

The result is

$$\begin{aligned} &\frac{1}{x}\frac{\partial}{\partial x}\left[\frac{1}{\hat\rho x}\frac{\partial}{\partial x}(x^2\hat\rho\hat{Q}_{\theta r}) + \frac{1}{\hat\rho \sin\theta}\frac{\partial}{\partial\theta}(\sin\theta\hat\rho\hat{Q}_{\theta\theta}) \right.\\ &\qquad \left. + \hat{Q}_{r\theta} - \cot\theta\hat{Q}_{\phi\phi}\right] - \frac{1}{x}\frac{\partial}{\partial\theta}\left[\frac{1}{\hat\rho x^2}\frac{\partial}{\partial x}(x^2\hat\rho\hat{Q}_{rr}) \right.\\ &\qquad \left. + \frac{1}{\hat\rho x \sin\theta}\frac{\partial}{\partial\theta}(\sin\theta\hat\rho\hat{Q}_{r\theta}) - \frac{1}{x}\hat{Q}_{\theta\theta} - \frac{1}{x}\hat{Q}_{\phi\phi}\right] \\ &\qquad - \frac{\cos\theta \,\mathrm{Ta}}{2x}\frac{\partial}{\partial x}(x\hat{u}_\phi) + \frac{\mathrm{Ta}}{2x}\frac{\partial}{\partial\theta}(\sin\theta\hat{u}_\phi) = 0 . \qquad (35)\end{aligned}$$

The Taylor number (eq. 3) couples the centrifugal terms in equation (35) to the contributions of the turbulence-originated Reynolds stress. In contrast to equation (32), the latter are normalized here with ν_T^2/R^2.

The normalized components of the (symmetric) correlation tensor are

$$\hat{Q}_{rr} = -2 \frac{\partial}{\partial x}\left(\frac{1}{\hat{\rho} x^2 \sin\theta} \frac{\partial \hat{A}}{\partial \theta}\right),$$

$$\hat{Q}_{r\theta} = -\frac{\partial}{\partial x}\left(-\frac{1}{\hat{\rho} x \sin\theta} \frac{\partial \hat{A}}{\partial x}\right) - \frac{1}{x}\frac{\partial}{\partial \theta}\left(\frac{1}{\hat{\rho} x^2 \sin\theta}\frac{\partial \hat{A}}{\partial \theta}\right) + \frac{1}{x}\left(-\frac{1}{\hat{\rho} x \sin\theta}\frac{\partial \hat{A}}{\partial x}\right),$$

$$\hat{Q}_{r\phi} = -\frac{\partial \hat{u}_\phi}{\partial x} + \frac{1}{x}\hat{u}_\phi + \frac{1}{x}(V_0 + V_1 \sin^2\theta)\hat{\hat{u}}_\phi ,$$

$$\hat{Q}_{\theta\theta} = -\frac{2}{x}\frac{\partial}{\partial \theta}\left(-\frac{1}{\hat{\rho} x \sin\theta}\frac{\partial \hat{A}}{\partial x}\right) - \frac{2}{x}\left(\frac{1}{\hat{\rho} x^2 \sin\theta}\frac{\partial \hat{A}}{\partial \theta}\right),$$

$$\hat{Q}_{\theta\phi} = \frac{\cot\theta}{x}\hat{u}_\phi + \frac{\cot\theta}{x} H_1 \sin^2\theta\, \hat{\hat{u}}_\phi - \frac{1}{x}\frac{\partial \hat{u}_\phi}{\partial \theta},$$

$$\hat{Q}_{\phi\phi} = -\frac{2\cot\theta}{x}\left(-\frac{1}{\hat{\rho} x \sin\theta}\frac{\partial \hat{A}}{\partial x}\right) - \frac{2}{x}\left(\frac{1}{\hat{\rho} x^2 \sin\theta}\frac{\partial \hat{A}}{\partial \theta}\right). \tag{36}$$

Stress-free boundary conditions are imposed at the top and bottom of the convection zone, i.e.,

$$\hat{A} = 0\,, \quad \hat{Q}_{r\theta} = 0\,, \quad \hat{Q}_{r\phi} = 0\,. \tag{37}$$

With the definition in equation (34) and after our normalization procedure, it makes sense to fix the azimuthal velocity at the equator to zero:

$$\hat{u}_\phi \Big|_{\rm eq} = 0\,. \tag{38}$$

4. RESULTS

In what follows, results of the numerical solution of equations (22) and (23) are presented. First, the turbulence parameters V_0, V_1, and H_1 are fixed in accordance with equation (15). The Taylor number remains as the only free parameter defining slow and fast rotation.

In § 4.2, more turbulence theory is added. Both the complete Λ effect and the eddy viscosity (tensor) can be derived for a given turbulence model under the influence of a given basic rotation. The known expressions are derived in the frame of a certain quasilinear approximation, so that the corresponding expressions are not perfect.

Rather, they are functions of the Coriolis parameter Ω^*, which now must be considered as the basic parameter. Therefore, even the Taylor number is no longer a free parameter directing the flow regimes presented in § 4.2.

In all our calculations, the density stratification used in equations (31) and (35) is taken from the model of Stix & Skaley (1990). For the determination of the exponent n' in equation (8), it suffices to reproduce the solar situation with a well-chosen Taylor number or rotation rate and then to vary that parameter. In principle, one only needs three models, describing cases of slow, medium, and fast rotation, in order to derive the exponent n' in equation (8).

4.1. *Variation of the Taylor Number for Fixed* Λ

We start with the highly simplified model. The Λ effect as generator of the nonuniform rotation *is fixed* to the values given in equation (15). Figure 1 gives the "solar" case, with $\delta_{\rm lat} \simeq 0.3$ at the surface. The meridional drift is poleward, with an amplitude of about 7 m s^{-1}. Figure 3 presents the same model but with a smaller Taylor number (Ta = 10^3). The normalized differential rotation is increased, and the drift is decreased. The opposite is true for a higher Taylor number (Fig. 4). Obviously, *the meridional flow tends to smooth the surface rotation profile*. Indeed, the exponent n' in equation (8) proves to be positive (Fig. 5). If the observations provide positive n', then after our calculations this could easily reflect the influence of the meridional flow induced by the Λ effect. Note that there is even a quantitative agreement with the observations. A value of about 0.15–0.30 can indeed be found in the vicinity of the Taylor number used here for the "solar" case.

Adopting solar values for the normalization of the meridional flow at the surface ($v_T/R \simeq 1$ m s^{-1}), we find for the solar case (Fig. 1) about 7 m s^{-1}, which value is increased for faster rotation. In Figure 4, using a Taylor number of Ta $= 10^7$, one finds a meridional drift of 15 m s^{-1}, which is in excess of the observational limit for the Sun.

4.2. *Variation of the Coriolis Number*

One might be unsatisfied by the simplicity of the model represented by Figures 1–5. Of course, the Taylor number and the Λ effect both depend on the basic rotation rate Ω. Actually, faster rotation also increases the Coriolis number Ω^*, so that both the Λ effect and the Taylor number are changed by changing Ω^*. The related expressions are given by equations (16)–(21) and, for the Taylor number, by equation (5). Therefore, in the following analysis only the Coriolis number will be varied. However, this results in the alteration of the eddy viscosity. In Kitchatinov et al. (1994), the structure of the eddy viscosity tensor under the influence of a global rotation is derived within the framework of a quasilinear theory. The tensor becomes highly anisotropic, making the theory more complicated. In the present paper, we apply only the Ω dependence of the isotropic part of the viscosity tensor, i.e., the coefficient of the deformation tensor, replacing equation (4) by

$$\nu_T = \nu_0\, \phi_1(\Omega^*)\,, \tag{39}$$

with

$$\nu_0 = \frac{c_\nu\, l_{\rm corr}^2}{\tau_{\rm corr}} \tag{40}$$

and

$$\phi_1 = \frac{15}{128\Omega^{*4}}\left(-21 - 7\Omega^{*2} + \frac{8\Omega^{*4}}{1+\Omega^{*2}} + \frac{\Omega^{*4} + 14\Omega^{*2} + 21}{\Omega^*} \arctan\Omega^*\right). \tag{41}$$

Again, as in equation (18), we adopt

$$\frac{l_{\rm corr}}{R} \simeq \frac{\alpha_{\rm MLT}}{\gamma}\frac{H_\rho}{R} \simeq \frac{\alpha_{\rm MLT}}{\gamma}\,\xi\,. \tag{42}$$

For reference, the computation starts with the artificial case of Ta $= 0$ (Fig. 6), i.e., completely neglecting the angular momentum transport of meridional circulation. We have used larger $\alpha_{\rm MLT}$ to increase the differential rotation. Again, $\gamma = 5/3$, $\xi = 0.1$, and $c_\nu = 1$. Except in the equatorial region, the isoline contours of the angular velocity agree with results from helioseismology. Of course, the flow pattern is far from that produced in the Taylor-Proudman regime. The surface pole-equator difference of the angular velocity is about 50%.

Let us proceed to the inclusion of the meridional flow. In Figures 7, 8, and 9, the Coriolis number Ω^* runs from 1 to 5, and the corresponding differential rotation profile changes drastically. Solar-type rotation is realized for $\Omega^* = 2$, leading to a Taylor number of $\simeq 2 \times 10^5$. The surface pole-equator difference of the angular velocity is reduced by the action of the meridional flow to about 20%.

Slower rotation ($\Omega^* = 1$, Ta $\simeq 8 \times 10^3$) yields spherical isolines of the rotation rate (Fig. 7). Faster rotation ($\Omega^* = 5$, Ta $\simeq 2 \times 10^7$) basically produces the two-dimensional Taylor-Proudman status (Fig. 9). In this case, equator and midlatitudes are rotating with nearly the same angular velocity. However, we do not see a polar vortex (i.e., a situation in which the poles rotate faster than the equator). This may be a consequence of the turbulence model used, that of Kitchatinov & Rüdiger (1993), or of a neglect of thermodynamics, i.e., ignorance of rotationally reduced anisotropy in the eddy heat transport (cf. Kitchatinov & Rüdiger 1995).

For increasing Ω^*, the pole-equator difference of the angular velocity at the surface grows to a maximum of 20% for $\Omega^* \simeq 2.25$ and $c_\nu = 1$ (Fig. 10). The maximum magnitude is defined by our choice of the turbulence model parameters $\alpha_{\rm MLT}$ and $l_{\rm corr}$, as well as the scaling factor c_ν. On its slow-rotation side, $n' \simeq -1$. Beyond the maximum, on the fast-rotation side, the differential rotation is reduced by the meridional flow. Accordingly, the scaling exponent n' changes its sign from negative for slow rotation to positive for fast rotation. In the latter case, the exponent n' adopts values of 0.4 for Coriolis numbers up to ~ 4, and might grow further for faster rotation. Hence, a population of young stars should behave quite differently with respect to surface differential rotation than a sample of very old stars. This is implied observationally by Donahue (1993).

The profiles in Figure 10 yield the only possibility for tuning the scaling factor c_ν in the definition of the eddy viscosity in equation (4). The value $c_\nu = 1$ may be considered as maximal. In Figure 10, the result for a smaller value is also given. The smaller the value of the proportional constant, the earlier the maximal (normalized) differential rotation appears in a run of increasing rotation rates. As the rotational influence on the eddy heat transport becomes nonnegligible, in particular for fast rotation, the development of a much more complex theory becomes necessary.

REFERENCES

Baliunas, S. L., et al. 1995, ApJ, 438, 269
Brandenburg, A., Moss, D., Rüdiger, G., & Tuominen, I. 1990, Solar Phys., 128, 243
Donahue, R. 1993, Ph.D. thesis, New Mexico State University
Donahue, R. A., & Baliunas, S. L. 1992, ApJ, 393, L63
———. 1994, in ASP Conf. Ser. 64, Cool Stars, Stellar Systems and the Sun, ed. J.-P. Caillault (San Francisco: ASP), 396
Donahue, R. A., Saar, S. H., & Baliunas, S. L. 1996, ApJ, 466, 384
Frisch, U., She, Z. S., & Sulem, P.-L. 1987, Physica, 28D, 382
Gray, D. F., & Baliunas, S. L. 1997, ApJ, 475, 303
Hathaway, D. H. 1996, ApJ, 460, 1027
Kitchatinov, L. L., Pipin, V. V., & Rüdiger, G. 1994, Astron. Nachr., 315, 157
Kitchatinov, L. L., & Rüdiger, G. 1993, A&A, 276, 96
———. 1995, A&A, 299, 446
Kitchatinov, L. L., Rüdiger, G., & Khomenko, G. A. 1994, A&A, 287, 320
Köhler, H. 1969, Ph.D. thesis, Univ. Göttingen
Küker, M., Rüdiger, G., & Kitchatinov, L. L. 1993, A&A, 279, L1
Rüdiger, G. 1989, Differential Rotation and Stellar Convection: Sun and Solar-Type Stars (New York: Gordon & Breach)
Rüdiger, G., & Kitchatinov, L. L. 1996, ApJ, 466, 1078
Rüdiger, G., & Tuominen, I. 1990, in IAU Symp. 138, Solar Photosphere: Structure, Convection, and Magnetic Fields, ed. J. O. Stenflo (Dordrecht: Kluwer), 315
Snodgrass, H. B., & Dailey, S. B. 1996, Sol. Phys., 163, 21
Stix, M., & Skaley, D. 1990, A&A, 232, 234
Tassoul, J.-L. 1978, Theory of Rotating Stars (Princeton: Princeton Univ. Press)
von Rekowski, B., & Rüdiger, G. 1997, in preparation